

High expression of BMP pathway genes distinguishes a subset of atypical teratoid/rhabdoid tumors associated with shorter survival

Diane K. Birks, Andrew M. Donson, Purvi R. Patel, Christopher Dunham, Andrea Muscat, Elizabeth M. Algar, David M. Ashley, B. K. Kleinschmidt-DeMasters, Rajeev Vibhakkar, Michael H. Handler, and Nicholas K. Foreman

Department of Neurosurgery, Anschutz Medical Campus, University of Colorado at Denver, Aurora, Colorado (D.K.B., B.K.K.-D., M.H.H.); Department of Pediatrics, Anschutz Medical Campus, University of Colorado at Denver, Aurora, Colorado (A.M.D., P.R.P., R.V., N.K.F.); Departments of Pathology and Neurology, Anschutz Medical Campus, University of Colorado at Denver, Aurora, Colorado (B.K.K.D.); The Children's Hospital, Denver, Colorado (D.K.B., A.M.D., P.R.P., R.V., M.H.H., N.K.F.); Division of Anatomic Pathology, Children's and Women's Health Centre of B.C., Vancouver, British Columbia, Canada (C.D.); Children's Cancer Centre Research Laboratory, Murdoch Children's Research Institute, Royal Children's Hospital, Parkville, Australia (A.M., E.M.A., D.M.A.); Department of Paediatrics, University of Melbourne, Royal Children's Hospital, Parkville, Australia (E.M.A., D.M.A.)

Molecular profiling of tumors has proven to be a valuable tool for identification of prognostic and diagnostic subgroups in medulloblastomas, glioblastomas, and other cancers. However, the molecular landscape of atypical teratoid/rhabdoid tumors (AT/RTs) remains largely unexplored. To address this issue, we used microarrays to measure the gene expression profiles of 18 AT/RTs and performed unsupervised hierarchical clustering to determine molecularly similar subgroups. Four major subgroups (clusters) were identified. These did not conform to sex, tumor location, or presence of monosomy 22. Clusters showed distinct gene signatures and differences in enriched biological processes, including elevated expression of some genes associated with choroid plexus lineage in cluster 4. In addition, survival differed significantly by cluster, with shortest survival (mean, 4.7 months) in both clusters 3 and 4, compared with clusters 1 and 2 (mean, 28.1 months). Analysis showed that multiple bone morphogenetic protein

(BMP) pathway genes were upregulated in the short survival clusters, with *BMP4* showing the most significant upregulation (270-fold). Thus, high expression of BMP pathway genes was negatively associated with survival in this dataset. Our study indicates that molecular subgroups exist in AT/RTs and that molecular profiling of these comparatively rare tumors may be of diagnostic, prognostic, and therapeutic value.

Keywords: Atypical teratoid/rhabdoid tumor, BMP4, bone morphogenetic protein pathway, microarray, survival.

Rhabdoid tumors are extremely aggressive tumors that occur primarily in young children. These tumors can occur in kidney, extra-renal tissues, or the central nervous system (CNS). Those that occur in the CNS are specifically referred to as atypical teratoid/rhabdoid tumors (AT/RTs). Histologically, rhabdoid tumors are generally recognized by the presence of rhabdoid cells and by expression of markers from heterogeneous cell lineages in a single tumor.¹ Molecularly, it has been shown that the hallmark of rhabdoid tumors is deletion or mutation of the gene *SMARCB1* (aka *INI1*, *hSNF5*, *BAF47*) that results in loss of functional protein expression.^{2,3}

Received March 24, 2011; accepted July 25, 2011.

Corresponding Author: Diane K. Birks, University of Colorado, Denver–Anschutz Medical Campus, Department of Neurosurgery, Mail Stop 8302, PO Box 6511, Aurora, CO 80045 (diane.birks@ucdenver.edu)

Although progress has been made in treating other World Health Organization grade IV CNS tumors, such as medulloblastoma, AT/RTs have a dismal prognosis, with typical survival times of <2 years, even with aggressive treatment.⁴ Gross total resection and use of radiation in children aged >3 years have been associated with improved survival times.^{5,6} Recently, use of intensive multimodal treatment based on a rhabdomyosarcoma protocol has shown an increase in survival (2-year overall survival rate, 70% \pm 10%).⁷ To date, only 2 factors aside from treatment have been found to be prognostic for outcome in AT/RTs. Younger age at diagnosis (<2 or 3 years)^{4,8} and the presence of germline mutations^{9,10} are associated with shorter survival times.

Studies of medulloblastoma and gliomas have shown that, even within a single diagnostic entity, individual tumors can be subclassified into different groups based on their gene expression.^{11–17} Classification based on this molecular profiling may show higher prognostic accuracy than histopathological or clinical criteria.^{18,19} In addition, these underlying biological differences may affect treatment responses. Therefore, recognition of tumor subgroups based on molecular profiling can provide important guidance for evaluation of treatments and development of new therapies. For AT/RTs, it has been suggested that differences in AKT phosphorylation may define tumor subgroups.²⁰ However, analysis of global gene expression in AT/RTs has only been conducted in studies using 5, 9, and 3 samples.^{16,21,22} Understandably, no attempt has been made to identify molecular subgroups with use of these limited datasets. Thus, the extent to which gene expression may vary among AT/RTs remains unexplored.

Our aim in the study reported here was to examine the molecular profiles of AT/RTs to determine whether prognostic or diagnostic subsets exist in this diagnostic entity, as have been identified in other tumors. Toward this goal, we used microarray technology to measure the expression of ~20,000 distinct genes in 18 AT/RT tumor samples, which represents the largest collection of gene expression data reported to date for this tumor type. With use of these data, unsupervised hierarchical clustering was performed to determine molecularly similar subgroups. The subgroups were analyzed to identify the biological processes and signaling pathways associated with each. Of importance, subgroups were also analyzed for differences in overall survival. The results presented in this study are the first to address whether subclassifications with prognostic or diagnostic use may exist in AT/RTs.

Materials and Methods

Tumor Specimens

A total of 18 AT/RTs were included in this study. Fourteen specimens were from patients who underwent surgical procedures at The Children's Hospital, Denver, Colorado, from 1995 through 2010, in compliance with internal review board regulations (COMIRB #95-500). Nine of

these samples have been published elsewhere.²¹ Tumor samples were collected at the time of surgery and snap frozen in liquid nitrogen until further use. Additional specimens were from the Children's Cancer Centre, Royal Children's Hospital, Parkville, Australia (1 sample), and from the Children's and Women's Health Centre of BC, Vancouver, Canada (3 samples). All 18 AT/RT tumor samples were collected before initial treatment, and all showed homogeneous loss of nuclear immunostaining for SMARCB1 protein. Patient characteristics, including presence or absence of monosomy 22 by fluorescence in situ hybridization, are shown in Table 1.

Molecular Profiling by Gene Expression Microarray

Gene expression of samples was measured using Affymetrix HG-U133 Plus 2 GeneChip microarrays (Affymetrix). RNA was extracted from each sample with use of an RNeasy or DNA/RNA AllPrep kit (Qiagen), according to the manufacturer's directions. Five micrograms of RNA was then reverse-transcribed using a T7-(dT) 24 oligomer and Superscript II Reverse Transcriptase (Invitrogen). The resulting cDNA was converted to cRNA, fragmented, and labeled using the Enzo BioArray HighYield RNA transcript labeling kit (Enzo Life Sciences). For 1 sample (3161), limited amount of starting RNA precluded use of the Superscript II/Enzo protocol. Instead, 400 ng of RNA from sample 3161 was processed using the Ambion MessageAmp Premier RNA Amplification Kit (Applied Biosystems), according to the manufacturer's directions. RNA quality for all samples was verified using the Nano Assay Protocol for the 2100 Bioanalyzer (Agilent) at 2 times: (1) after initial extraction of the RNA from the tumor sample and (2) after preparation of the RNA for chip hybridization. The fragmented, labeled RNA was hybridized to the HG-U133 Plus 2 GeneChips, according to the manufacturer's instructions.

Data Analysis

Data analysis was performed in R (<http://www.r-project.org/>), using packages publicly available through Bioconductor (<http://www.bioconductor.org>). As a first step, the scanned microarray data were background corrected and normalized using the gcRMA algorithm²³ resulting in log 2 gene expression values. Multiple probe-sets for a gene were then collapsed to 1 entry per gene, based on the mean best-expressed probe-set for that gene. All subsequent analyses used these normalized values for input. CEL files and normalized microarray data have been deposited in GEO (accession number GSE28026).

Hierarchical clustering was performed using the normalized gene expression data. Distances based on Spearman correlations were calculated for input to an agglomerative algorithm with use of complete linkage, as implemented in the Bioconductor hclust function.

Differential gene expression between clusters was calculated using the Bioconductor limma function.²⁴ Data were filtered before input to eliminate genes not expressed

Table 1. Characteristics of the 18 patients with AT/RTs in this study

Sample ID	Sex	Location	Chromosome 22 monosomy	Age at diagnosis (months)	Survival time (months)	Status
Cluster 1						
413	M	posterior fossa	Y	46	10	DOD
514	M	parietal/occipital lobes	N	33	16	DOD
515	M	frontal lobe	N	17	42	Alive, NOD
3161	F	posterior fossa	N	30	36	Alive, NOD
Average				32	26	
Cluster 2						
504	M	posterior fossa	N	7	31	DOD
605	M	frontal lobe	Y	38	6	DOD
663	F	posterior fossa	Ring chromosome 22	22	10	DOD
737	M	posterior fossa	N	12	7	Alive, with recurrence
90004	F	posterior fossa	Y	17	101	Alive, NOD
90007	F	temporal	N	20	12	DOD
Average				19.3	27.8	
Cluster 3						
119	M	posterior fossa	Y	11	6	DOD
517	M	posterior fossa	Y	24	Unknown	Lost to follow-up
687	M	posterior fossa	?	16	1	DOC
Average				17	3.5	
Cluster 4						
3	F	posterior fossa	?	19	12	DOD
343	F	posterior fossa	?	0	1	DOD
370	F	posterior fossa	N	6	4	DOD
404	M	posterior fossa	Y	5	7	DOD
90005	M	posterior fossa	?	10	2	DOD
Average				8	5.2	

Chromosome 22 monosomy was assessed by fluorescence in situ hybridization. DOC, died of complications; DOD, died of disease; NOD, no evidence of disease.

in any samples or that showed only limited variance across samples. The limma function performs pair-wise comparisons between a target group and each of the other user-defined groups in the dataset. It uses an Empirical Bayes approach to calculate a moderated *t* statistic and calculates a false discovery rate (FDR) that accounts for multiple testing both within and across groups. The unique molecular signature of each cluster was defined as genes that showed significant differential expression in all 3 of the pair-wise comparisons (FDR ≤ 0.1 and mean fold difference ≥ 1.5) and for which the mean difference was in the same direction when compared with all of the other clusters (ie, either all upregulated or all downregulated in all of the comparisons with respect to that cluster).

The Kaplan-Meier method was used to estimate the probability of survival as a function of time. Survival was calculated from the date of initial diagnosis to the date of death from any cause; patients alive at the time of analysis were censored. Differences between survival curves were analyzed for significance with use of the log-rank test. Multivariate analysis of the relative importance of factors to survival was performed using the Cox proportional hazards method.

Differences between shorter survival and longer survival groups for individual genes were calculated using 2-sample *t* tests. The FDR was estimated using the Benjamini and Hochberg method, as implemented in the Bioconductor function *q* value. An FDR cutoff of ≤ 0.05 with a mean fold difference ≥ 1.5 was used to indicate significance.

Functional annotation analysis of differentially expressed genes was performed with the National Institutes of Health Database for Annotation, Visualization, and Integrated Discovery (DAVID) Web tool (<http://david.abcc.ncifcrf.gov/>),^{25,26} using Biological Process Gene Ontology (GO)²⁷ terms and Kyoto Encyclopedia of Genes and Genomes (KEGG) pathways. Gene set enrichment analysis was used to examine enrichment of genes in predefined reference sets that are based on biological knowledge.²⁸ Unlike other approaches that examine only genes meeting a predetermined cutoff, this tool computes an aggregate score for all genes in the reference set, based on their relative ranking in the data.

Functional network analysis was performed using Ingenuity Pathways Analysis (IPA; Ingenuity Systems; <http://www.ingenuity.com>), which enables the visualization and exploration of molecular interaction networks

on the basis of gene expression data. The genes showing statistically significant differences between shorter and longer survival groups, as identified above, were used as input. These genes were overlaid onto a global molecular network developed from information contained in Ingenuity's Knowledge Base. Networks were then algorithmically generated on the basis of their connectivity and were ranked by IPA on the basis of the number of genes represented in the network from the submitted gene list.

Quantitative Real-Time Polymerase Chain Reaction

Gene expression was validated using quantitative real-time polymerase chain reaction (qRT-PCR) performed on a StepOne Plus Real Time PCR System (Applied Biosystems) using Taqman gene assay reagents (Applied Biosystems), according to the manufacturer's protocols. First-strand cDNA was generated from total RNA with use of the High-Capacity cDNA kit (Applied Biosystems). The resulting cDNA was used as input to each qRT-PCR, along with the appropriate Taqman gene-specific probe and PCR reagents. All qRT-PCR assays were done in triplicate. Relative quantity was calculated using the $\Delta\Delta CT$ method with *GAPDH* as the endogenous control.

Results

Unbiased Hierarchical Clustering Identifies 4 Molecular Clusters in AT/RTs

To examine the molecular landscape of AT/RTs, gene expression of 18 AT/RTs was measured using Affymetrix U133 Plus2 GeneChips. Unsupervised hierarchical clustering was performed using only the genes with the highest variance across samples (top 10%). In the resulting dendrogram, the AT/RTs are grouped into 4 main clusters, with 4 samples in cluster 1, 6

samples in cluster 2, 3 samples in cluster 3, and 5 samples in cluster 4 (Fig. 1A). To test the robustness of this grouping, clustering was repeated using different cutoff values (eg, top 20%, top 50%, or top 70% of genes). Only one change occurred in any of the clustering outcomes: sample 737 switched from cluster 2 to cluster 3. The remainder of the results remained identical regardless of the number of genes on which clustering was based (data not shown). These results indicate that these cluster groupings are highly stable and robust for this dataset. The subgroups were further examined by principal components analysis. Cluster 1 and cluster 4 showed clear separation from each other and the other clusters (Fig. 1B). Clusters 2 and 3 showed more proximity to each other, but still appeared as separate groups. Thus, the principal components analysis results are consistent with the clustering results. All subsequent analyses were performed using the cluster assignments shown in Fig. 1A. The patient characteristics for the samples included in this study, grouped by cluster, are shown in Table 1. These data show that the clusters are not based on sex, location of tumor, or presence of monosomy 22.

Molecular Clusters Show Distinct Gene Expression

Differential expression was examined to determine which genes were most distinctive for each cluster. Cluster 4 showed the most unique gene signature, with 531 genes differentially expressed, compared with clusters 3, 2, and 1. Cluster 2 contained 346 signature genes, compared with 4, 3, and 1, whereas cluster 3 and cluster 1 showed the fewest differences, with only 81 and 201 genes, respectively (Supplementary Table 1). Of note, several genes associated with choroid plexus, including *TTR*, *KCNJ13*, *HTR2C*, and *F5*,²⁹ were significantly upregulated in cluster 4. However, other genes associated with choroid plexus in the same study, such

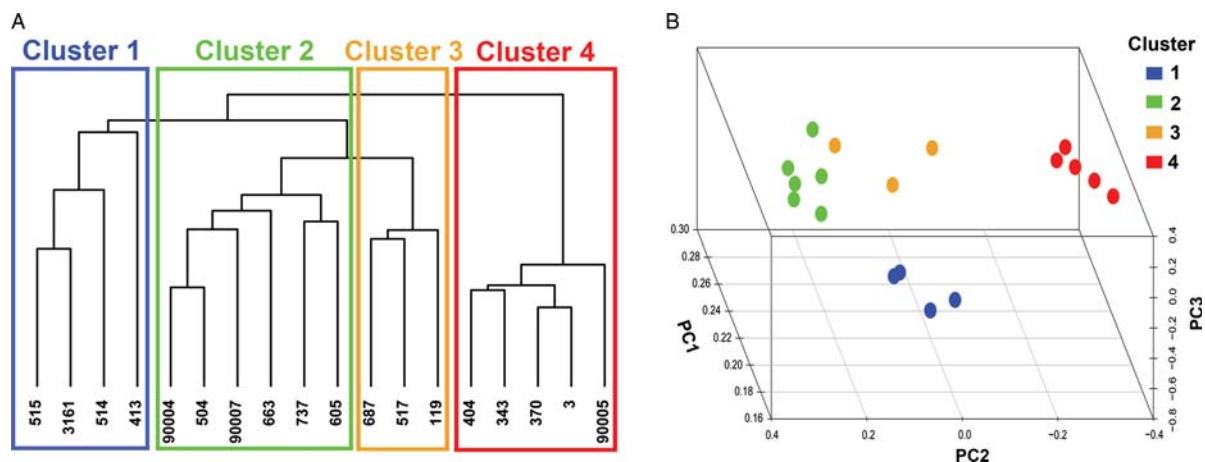


Fig. 1. Hierarchical clustering of AT/RTs. (A) Molecular profiling was performed using gene expression microarrays to measure 19,667 genes in 18 AT/RT tumor samples. The top 10% of genes, as ranked by variance across samples, were used as input to an agglomerative hierarchical clustering algorithm. Four clusters are defined on the resulting dendrogram, marked clusters 1–4. (B) Principal component analysis (PCA) of the AT/RTs in (A) using the same top 10% of high variance genes in (A).

as *STC*, *GPX3*, and *FBLN1*, did not show any difference in expression across clusters.

To further characterize each cluster, the Web tool DAVID was used to look for enrichment of genes associated with GO biological process terms or KEGG pathways. The signature genes identified above for each cluster were input to DAVID. Results show that distinct processes were enriched in each cluster (Supplementary Table 2). In cluster 1, immune response-related processes were enriched among upregulated genes, represented most frequently by *IL18*, *TLR4*, *GIMAP5*, and *CASP1*. Bone development processes were associated with down-regulated genes in cluster 1, including *BMP2*, *BMP7*, and *FZD1*. Numerous processes related to neurogenesis and transcriptional regulation were upregulated in cluster 2. Sixty-three upregulated genes in cluster 2 contributed to enrichment of these processes, including *APBB1*, *ASCL1*, *GL2*, *ID4*, *PBX1*, and *POU3F1*. Various immune processes related to HLA genes were downregulated in cluster 2. Cluster 3 showed upregulation of 3 genes (*CFC1*, *RTTN*, and *SHH*) associated with establishment of left-right symmetry. Cluster 4 showed upregulation of WNT-signaling pathway genes, including *FZD6*, *FZD9*, and *WNT5A*. Finally, in contrast with cluster 2, cluster 4 showed that numerous processes related to neurogenesis, brain development, and axonogenesis are associated with 26 down-regulated genes, including *CDH4*, *MAP1B*, *NTN1*, *POU3F2*, *ROBO1*, and *TIAM1*.

AT/RT Molecular Clusters Show Partial Correspondence to Histological Observations

To determine whether there are any histological correlates to the molecular clusters, pathology reports were reviewed for the samples in this study. Pathology reports, all based on surgical sections, were available for 14 of the 18 tumors. Observed tumor histopathology showed some correspondence to the molecular clustering, as noted below.

Gross cell morphology was distinct for samples in cluster 2, compared with other clusters. Small, monotonous blue cells were the primary component in all of the 4 tumors for cluster 2. No rhabdoid cells were observed in 2 of these tumors. In contrast, none of the 10 samples across clusters 1, 3, or 4 contained a predominant blue cell component.

One tumor in cluster 3 and 1 tumor in cluster 4 were originally diagnosed as choroid plexus carcinomas. Subsequent to the establishment of nuclear loss of SMARCB1 protein as a marker for AT/RTs, these tumors were re-analyzed with this immunostain. Both tumors showed loss of SMARCB1 and were subsequently reclassified as AT/RTs. An additional tumor in cluster 4, although recognized as an AT/RT because of loss of SMARCB1 immunostaining throughout the tumor, was noted to have a distinct papillary architectural pattern suggestive of choroid plexus lineage. These findings are of note because of the upregulation of choroid plexus-related genes observed by molecular profiling in cluster 4.

Differences in proliferation rate also appeared to vary by cluster. Samples in cluster 4 were associated with the highest proliferation rates, as measured by ≥ 6 mitoses observed per high power (40x) field and/or positive immunostaining by MIB1 (seen only in cells in G1, S, or M phase of cell cycle) in 40%–60% of tumor cells. Samples in clusters 1, 2, and 3 showed proliferation rates of 3 mitoses per high power field or $\leq 40\%$ cells positive for MIB1.

Immunohistochemistry for mesenchymal (vimentin, smooth muscle actin), epithelial (pan-cytokeratin, epithelial membrane antigen), glial (glial fibrillary acidic protein), and neuronal (synaptophysin, neurofilament protein, and neuron-specific enolase) lineage markers did not show any consistent differences between clusters.

AT/RT Molecular Clusters Are Differentially Associated with Survival

Past studies have shown that molecular profiling of tumors may identify subgroups with prognostic differences, in addition to molecular differences. Therefore, overall survival was analyzed for the identified AT/RT clusters. A Kaplan-Meier plot shows that the 4 clusters differed significantly with respect to survival ($P < .001$) (Fig. 2A). Shorter overall survival times were seen for clusters 3 and 4, whereas clusters 1 and 2 showed longer survival. Mean survival times for clusters 1–4 were 26.0, 27.8, 3.5, and 5.2 months, respectively. No significant survival difference existed between clusters 3 and 4 ($P = .55$) or between clusters 1 and 2 ($P = .48$). When all patients in clusters 3 and 4 were combined and analyzed as a single group, compared with all patients in clusters 1 and 2 combined as a single group, survival difference was highly significant ($P < .001$). Mean overall survival for clusters 3 and 4 combined was 4.7 months compared with 27.1 months for clusters 1 and 2 combined.

Age at diagnosis has been previously reported as a prognostic factor in AT/RTs.^{4,8} Therefore, our data were examined to determine whether diagnostic age was associated with overall survival time in our cohort. For the 18 patients in this study, mean age at diagnosis is 18.1 months. When divided into 2 groups based on this mean, no significant difference in overall survival was found for patients who received a diagnosis at age > 18 months, compared with those who received a diagnosis at age ≤ 18 months ($P = .71$). Dividing by older or younger than 3 years of age at diagnosis, a cutoff that has been used previously,⁴ was also not significant ($P = .72$). However, our dataset included only 2 patients > 3 years of age at diagnosis and, therefore, provided little basis for comparison. Multivariate analysis (Cox regression analysis) of cluster membership and age at diagnosis of > 36 months showed that cluster membership is an independent significant variable for overall survival ($P < .001$) (Fig. 2B).

Genes Associated with BMP Signaling Are Significantly Upregulated in AT/RT Clusters with Shorter Survival

Gene signatures associated with individual clusters were previously presented. However, shorter survival was

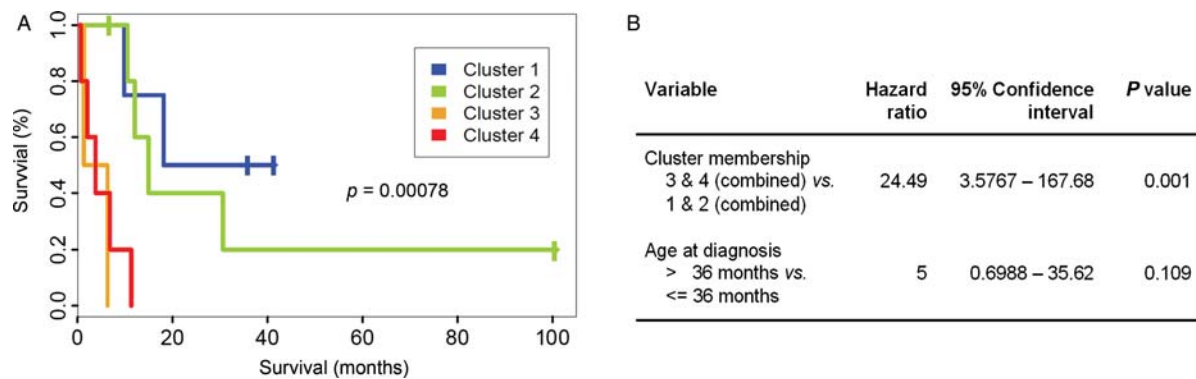


Fig. 2. Survival analysis of AT/RTs based on molecular classification. (A) Kaplan-Meier survival plot of 17 patients with AT/RT, using the clusters identified by hierarchical clustering of 18 patients with AT/RT (see Fig. 1). One patient included in the clustering was lost to follow-up and is not included in the survival analysis. The difference between the 4 clusters was statistically significant (log rank P value $< .001$). Vertical ticks indicate censored survival observations. (B) Multivariate survival model (Cox regression analysis) was used with the same patients in (A) to assess the importance of cluster membership and diagnostic age in AT/RT survival.

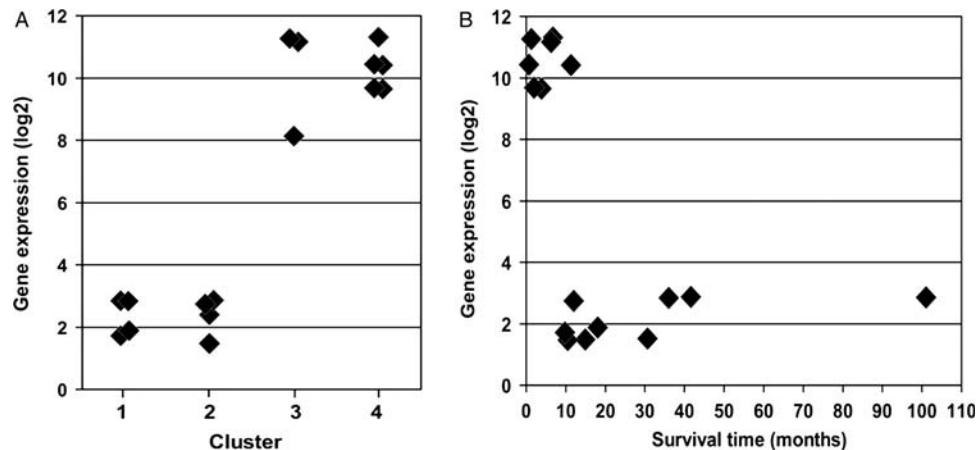


Fig. 3. *BMP4* gene expression in AT/RT samples. (A) Expression of *BMP4* mRNA in 18 AT/RT samples grouped by the molecular clusters defined in Fig. 1. Gene expression was measured by Affymetrix U133 Plus2 GeneChips. (B) The same *BMP4* expression values as (A), plotted against survival time for the 17 patients included in the survival analysis (Fig. 2) (one patient was lost to follow-up).

associated with both clusters 3 and 4, whereas both clusters 1 and 2 showed longer survival times. Therefore, to determine molecular signatures associated with survival, additional analysis was performed to identify genes differentially expressed among all samples in clusters 3 and 4 (hereafter referred to as the short survival group) compared with all samples in clusters 1 and 2 (hereafter referred to as the longer survival group).

Overall, 193 genes were differentially expressed between these 2 groups (Supplementary Table 3). A total of 97 genes were upregulated in the short survival group. The top upregulated gene was *BMP4* (FDR = 1.3×10^{-8}), with a mean expression 270-fold higher in the short survival group. *BMP4* showed little to no expression in the longer survival group (Fig. 3A). When plotted against survival time, high *BMP4* expression was consistently associated with short survival times, whereas low *BMP4* was associated with a broad range of survival times (although generally longer than those with high *BMP4*) (Fig. 3B).

DAVID was used to look for enrichment of genes annotated in GO biological process terms or KEGG pathways. Processes enriched among upregulated genes in the short survival group included RAS signaling, tube development, and embryonic development (Table 2). Additional processes enriched among upregulated genes included negative regulation of apoptosis ($P = .01$), muscle development ($P = .024$), and skeletal development ($P = .025$). The upregulated genes in the short survival group that contributed most frequently to enrichment of functions included *BMP4*, *MSX1*, *EDN1*, *GATA6*, *IGF1*, *ALS2*, and *TFAP2A*. Of note, many of the genes listed in the enriched processes are involved with BMP signaling, including *BMP4*, *MSX1*, *EDN1*, *GATA6*, *GDF5*, and *SOST*.

To further explore the relevance of BMP pathway genes to differences in survival, 2 reference gene sets were created. The first set (GS#1) consisted of all genes annotated in Gene Ontology with the term GO:30509 – BMP signaling pathway (a total of 73 genes). Because this list

Table 2. Biological processes enriched in the AT/RT short survival group

Term	P value
UPregulated in Short Survivors vs. Longer Survivors	
GO:0046579~positive regulation of Ras protein signal transduction	.003
GO:0051057~positive regulation of small GTPase mediated signal transduction	.003
GO:0035295~tube development	.006
GO:0001763~morphogenesis of a branching structure	.007
GO:0043009~chordate embryonic development	.007
GO:0009792~embryonic development ending in birth or egg hatching	.008
GO:0007167~enzyme linked receptor protein signaling pathway	.008
DOWNregulated in Short Survivors vs. Longer Survivors	
GO:0030182~neuron differentiation	<.001
GO:0031175~neuron projection development	<.001
GO:0030030~cell projection organization	<.001
GO:0048812~neuron projection morphogenesis	<.001
GO:0007411~axon guidance	<.001
GO:0048858~cell projection morphogenesis	<.001
GO:0048666~neuron development	<.001
GO:0032990~cell part morphogenesis	<.001
GO:0048667~cell morphogenesis involved in neuron differentiation	<.001
GO:0000904~cell morphogenesis involved in differentiation	.001
GO:0000902~cell morphogenesis	.002
GO:0006928~cell motion	.002
GO:0007409~axonogenesis	.002
GO:0032989~cellular component morphogenesis	.003
GO:0008284~positive regulation of cell proliferation	.004
GO:0045664~regulation of neuron differentiation	.004
GO:0044271~nitrogen compound biosynthetic process	.005
GO:0050767~regulation of neurogenesis	.009
GO:0048589~developmental growth	.009

Enrichment of biological processes among genes differentially expressed in the short survival group (clusters 3 and 4) compared with the longer survival group (clusters 1 and 2) was examined using the Web-based DAVID bioinformatics tool. The set of up- or downregulated genes was input into DAVID for functional analysis using the categories "Gene Ontology Biological Processes" and "KEGG Pathways." Processes with enrichment *P* value <.01 and containing at least 3 genes are listed.

contained significant omissions based on recent published research, a second list was also created. The second reference gene set (GS#2) consisted of all genes in the first set, augmented with additional genes known to be directly associated with the BMP signaling pathway based on recent reviews and published literature, for a total of 97 genes. Gene set enrichment analysis was used to determine whether the genes in either GO:30509 or the augmented BMP pathway list were enriched among upregulated genes in the short survival group. Significant enrichment was detected for both GS#1 (FDR = 0.014) and GS#2 (FDR = 0.014) (Supplementary Table 4). To identify all

BMP pathway-related genes dysregulated between the short survival and longer survival groups, expression for all genes in the augmented list (GS#2) was examined. Of the 87 genes in the list included on the microarray platform used in this study, 25 (29%) were dysregulated ($P < .05$), 18 were upregulated, and 7 were downregulated in the short survival group compared with the longer survival group (Fig. 4). Two additional genes (*ID1* and *FSTL1*) showed a strong trend toward upregulation ($P = .06$). Ligands *BMP4*, *GDF5*, *GDF11*, and *GDF15* and direct transcriptional targets *MSX1*, *MSX2*, *ID1*, *ID3*, *BAMBI*, *SMAD6*, *SMAD7*, and *SOST* were among the upregulated genes. Receptor *BMPRI1B* and transcriptional target *ID4* were among the downregulated genes.

To gain additional insight into the molecular differences between the short and longer survival groups, Ingenuity pathway analysis was used to identify interaction networks in the differentially expressed genes. The top network (Fig. 5) showed multiple linked signaling pathways revolving around *BMP4*, reiterating the results of gene function analysis and emphasizing the wide-ranging effects of BMP signaling in these tumors.

Genes Associated with Neuron Development and Differentiation Are Significantly Downregulated in Clusters with Shorter Survival

Ninety-six genes were significantly downregulated in the short survival group compared with the longer survival group. *GLI2*, part of the SHH signaling pathway, was among the downregulated genes, as were 7 genes associated with the BMP pathway. Functional analysis using DAVID showed that downregulated genes in the short survival group were strongly associated with biological processes related to neuron differentiation and axonogenesis (Table 2). Genes *GLI2*, *FOXP1*, *POU3F2*, *LIFR*, *SEMA6A*, *STMN3*, *TUBB2A*, *BMPRI1B*, *ID4*, *CELSR2*, *NRXN1*, and *NTN1* are represented in these categories. Thus, longer survival is associated with a more specific neuronal signature, whereas shorter survival is associated with a signature common to early development of many tissues.

Expression of Key BMP Signaling Genes Measured by qRT-PCR Validates and Extends Microarray Findings

To validate the microarray data, mRNA expression of 4 genes associated with BMP signaling was examined in a subset of tumor samples from across all clusters with use of qRT-PCR ($n = 5$). Results show ~300-fold higher expression of *BMP4* in samples from clusters 3 and 4 (short survival group) compared with those from clusters 1 and 2 (longer survival group) (Supplementary Fig. 1). A sixth sample from cluster 3 also showed 300-fold higher expression of *BMP4* by qRT-PCR (data not shown). Similarly, *SOST* and *MSX2*, both direct targets of BMP signaling, showed substantially higher expression in samples from clusters 3 and 4. *PCSK6*, required to create the active, cleaved form of *BMP4*, was also upregulated. Relative expression measured by

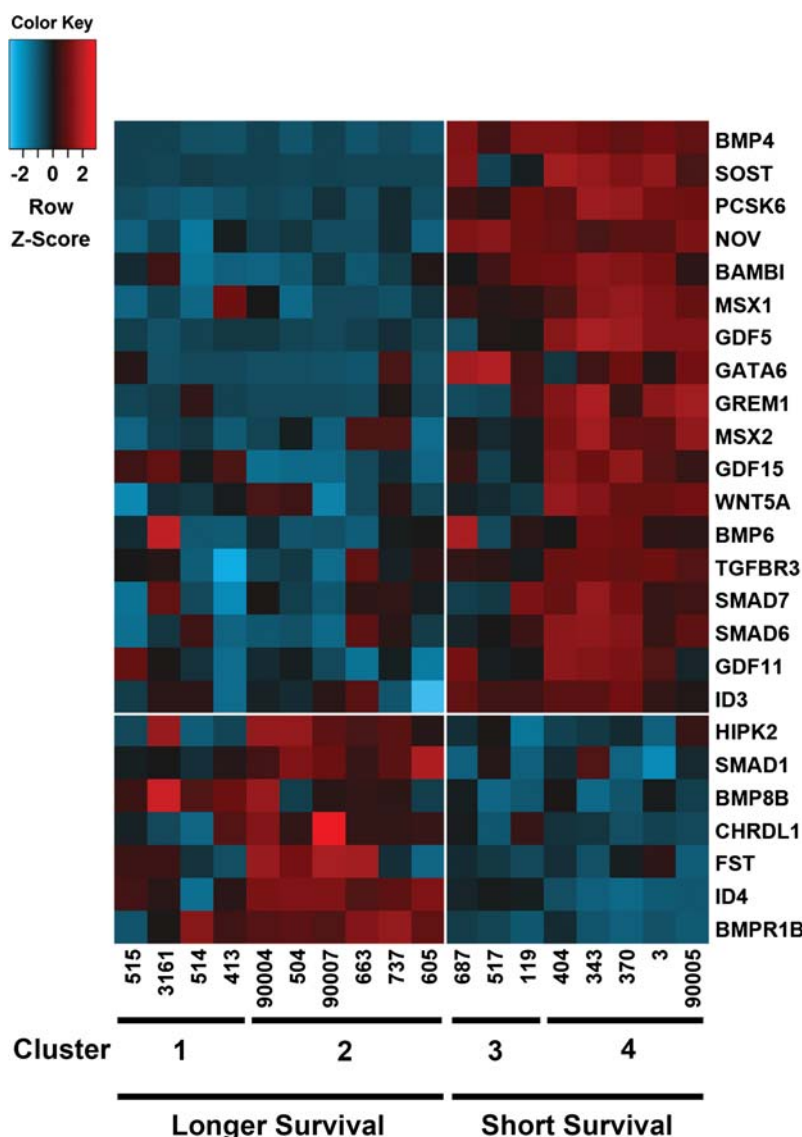


Fig. 4. Differentially expressed BMP signaling genes. Heatmap of expression data for all genes from BMP signaling geneset #2 that showed differential expression ($P < .05$) in clusters 3 and 4 (short survival group), compared with clusters 1 and 2 (longer survival group). Eighteen genes were upregulated, and 7 were downregulated. Gene expression was measured by Affymetrix U133 Plus2 GeneChips.

qRT-PCR for these genes correlated highly to the microarray expression (Pearson $r = 0.93-0.99$).

To extend our findings, 4 additional AT/RTs not included in the microarray analysis were analyzed by qRT-PCR for the above genes. Clinical characteristics of these additional samples are listed in Supplementary Table 5. One sample, 3074, showed high expression of *BMP4*, *SOST*, *MSX2*, and *PCSK6*, similar to that shown by samples in the short survival group; the other 3 samples showed very low expression of these genes, similar to that shown by samples in the longer survival group (Supplementary Fig. 2). Survival time for the patient with high expression was 2.5 months, consistent with the mean survival time in the short survival group of 4.7 months. Mean survival time for the 3 additional patients with low expression of these BMP-related genes was 27 months, with 2 patients still alive. This is consistent with the mean survival in the longer survival

group (27.1 months). Thus, these 4 additional patients showed a similar pattern of high BMP gene expression associated with shorter survival as seen in our original cohort of 18 patients.

Discussion

In this study, molecular profiling of AT/RTs was performed to determine whether distinct subgroups with therapeutic or prognostic relevance exist in this diagnostic category. With use of gene expression microarray data as input to an unbiased agglomerative hierarchical clustering algorithm, 4 clusters of AT/RTs were identified that showed differing gene expression profiles. This molecular clustering also corresponds with several observable histopathological features. Tumors composed predominantly of small blue cells with few or no observed

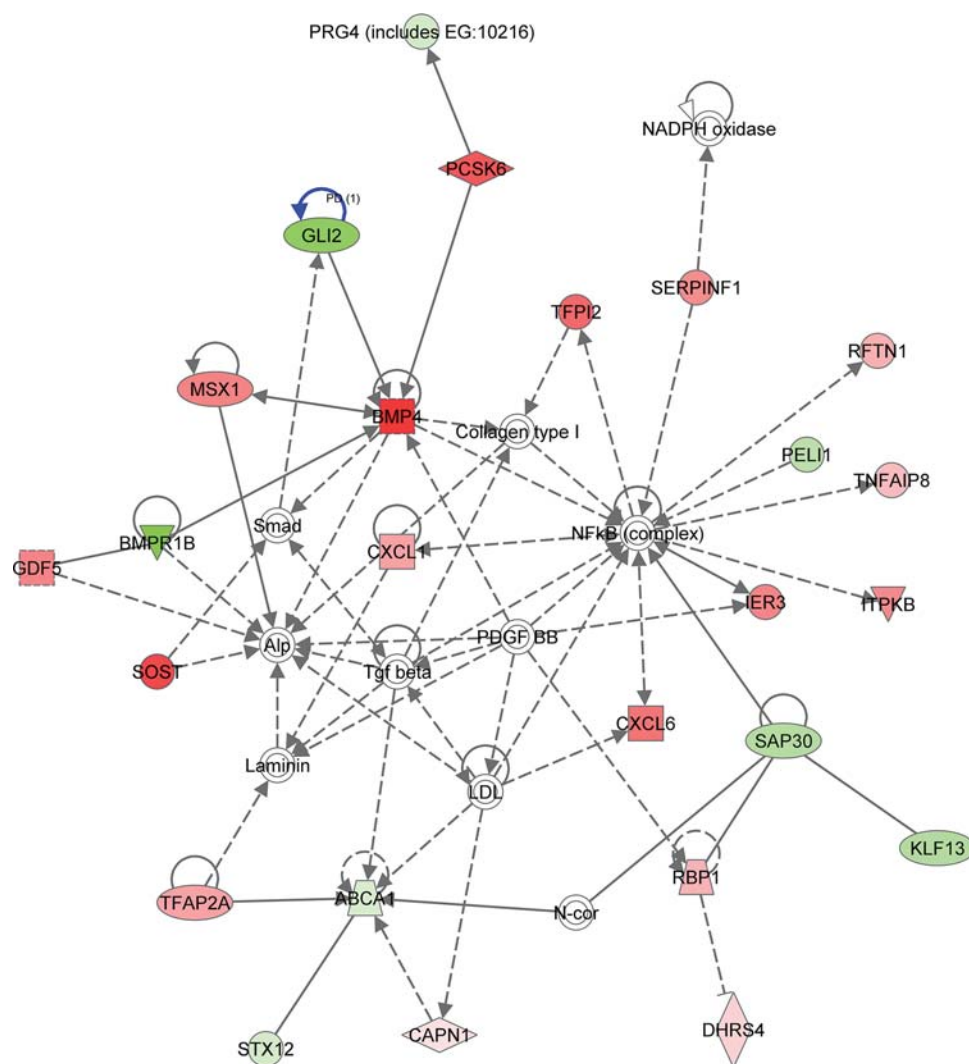


Fig. 5. Top-scoring Ingenuity pathways analysis functional network. The 193 genes differentially expressed between the short survival group (clusters 3 and 4) and the longer survival group (clusters 1 and 2) were input to Ingenuity pathway analysis for functional network generation. The top-scoring network is shown here. The intensity of the node color indicates the degree of upregulation (red) or downregulation (green) of genes differentially expressed in the dataset being examined.

rhabdoid cells grouped together in cluster 2 and showed significant upregulation of genes associated with neurogenesis. Cluster 4 tumors showed downregulation of genes associated with neurogenesis, brain development, and axonogenesis and higher proliferation rates (as measured by MIB1). Cluster 4 also showed specific upregulation of genes associated with choroid plexus epithelium, including transthyretin (*TTR*); potassium inwardly rectifying channel, subfamily J, member 13 (*KCNJ13*); 5-hydroxytryptamine (serotonin) receptor 2C (*HTR2C*); and coagulation factor V (*F5*).²⁹ The delineation between AT/RTs and choroid plexus tumors, particularly choroid plexus carcinomas, has long been a subject of debate.^{30–33} Our results suggest that, at least for some tumors, there is overlap at the gene expression level and at the histopathological level. This is also supported by a recent report showing membranous expression of *KCNJ13*, previously thought to be specific to tissues with choroid plexus lineage and found by us to

be upregulated in cluster 4, in 2 of 8 AT/RTs.³⁴ To our knowledge, our study is the first to find an association with this subset of AT/RTs and shorter survival.

In addition to different gene expression profiles, the clusters were associated with different overall survival times. Patients in clusters 3 and 4 experience significantly shorter overall survival than did those in clusters 1 and 2. Analysis of the differentially expressed genes indicates that upregulation of BMP pathway-related genes is strongly associated with shorter survival, with *BMP4* showing the most significant association. Although this study did not directly measure activation of BMP signaling, the upregulation of multiple direct gene targets is suggestive that BMP signaling is active in cluster 3 and 4 tumors.

BMP4 belongs to the TGF- β super-family of secreted growth factors. This super-family consists of 2 branches, the BMP/GDFs and the TGF- β /activin/nodal genes. BMP signaling elicits a wide diversity of transcriptional

programs and physiological responses that are highly variable both across different cell types and across signaling intensities. It plays a crucial role in normal development and maintenance of many tissues. In the brain, appropriate BMP signaling levels are critical to neural tube induction,³⁵ formation of neural crest cell populations,^{36,37} development of the dorsal-most forebrain including the choroid plexus,^{38,39} dorsal-ventral patterning of the spinal cord,^{40,41} cell-fate decisions in neural precursors,^{42,43} and generation and differentiation of cerebellar granule cells,^{44,45} among other processes.

The pleiotropic effects of BMP signaling are accomplished through 3 effectors: SMAD1, SMAD5, and SMAD8. SMADs are thought to exert their effects primarily through chromatin remodeling.^{46,47} SWI/SNF has been shown to be essential for transcription of several TGF- β and BMP downstream signaling targets.^{47–49} This raises the question of whether loss of the SWI/SNF component SMARCB1, as occurs in rhabdoid tumors, could affect BMP signaling.

In cancer, addition of BMP4 has been shown to down-regulate proliferation and promote cell differentiation in both a glioma cell line⁵⁰ and in Sonic hedgehog-driven models of medulloblastoma.⁵¹ On the other hand, BMP4 was overexpressed in malignant melanoma, where it promoted cell invasion and migration,⁵² thus reinforcing that effects of BMP signaling are highly dependent on cell context and other factors. For AT/RTs, it remains to be determined whether the upregulated BMP pathway gene expression seen in this study contributes to malignancy or is merely a marker of tumors with a different biological profile. Both differentiated choroid plexus cells and precursor cell populations, from which choroid plexus arises, are known to produce BMPs.^{39,53,54} Consistent with this, one of our molecularly defined clusters (cluster 4) showed both upregulated BMP expression and upregulation of genes normally associated with choroid plexus lineage.

Molecular profiling of CNS tumors has led to insights into signaling pathways that drive different subsets of these tumors and to identification of possible precursor cells for these tumors.^{55–57} In addition, multiple studies have identified gene signatures prognostic for survival in brain tumors.^{11,14–16,18} Most of these studies have analyzed 50–100 or more samples, and published data from other institutions have often been available for corroboration of results. In contrast, our research examines a

comparatively rare pediatric brain tumor and is based on a sample size of only 18 patients. There are currently no other published AT/RT gene expression data available for corroboration. Therefore, the findings presented here must be considered to be preliminary and will need to be evaluated further using additional patient cohorts. It would also be of interest to evaluate these findings in older patients, who are known to show better response to treatment,^{4,7,8} because our cohort included only 2 patients >3 years of age. In addition, this study is specific to AT/RTs (RTs of the brain) and did not assess RT tumors from other locations, particularly the kidney and soft tissues, which may show other molecular characteristics.

In conclusion, this study identifies molecular factors that define subsets of AT/RTs with distinct gene expression signatures. Our data indicate that, although loss of SMARCB1 is common to all of the AT/RTs studied, other differences in underlying biology distinguish subsets of these tumors, and these differences may affect overall survival under current therapeutic regimens. As with other pediatric brain tumors, molecular profiling of RTs is a promising avenue of research that may aid in the search for improved treatment strategies for this devastating disease.

Supplementary Material

Supplementary material is available online at *Neuro-Oncology* (<http://neuro-oncology.oxfordjournals.org/>)

Acknowledgements

Presented in part: Rhabdoid Tumors Working Group of the Children's Oncology Group, Dallas, TX, September 2010.

Conflict of interest statement. None declared.

Funding

This work was supported by The Morgan Adams Foundation.

References

- Louis DN. International Agency for Research on Cancer. World Health Organization. WHO classification of tumours of the central nervous system. 4th ed. Lyon: International Agency for Research on Cancer; 2007.
- Biegel JA, Tan L, Zhang F, Wainwright L, Russo P, Rorke LB. Alterations of the hSNF5/INI1 gene in central nervous system atypical teratoid/rhabdoid tumors and renal and extrarenal rhabdoid tumors. *Clin Cancer Res*. 2002;8(11):3461–3467.
- Judkins AR, Mauger J, Ht A, Rorke LB, Biegel JA. Immunohistochemical analysis of hSNF5/INI1 in pediatric CNS neoplasms. *Am J Surg Pathol*. 2004;28(5):644–650.
- Hilden JM, Meerbaum S, Burger P, et al. Central nervous system atypical teratoid/rhabdoid tumor: results of therapy in children enrolled in a registry. *J Clin Oncol*. 2004;22(14):2877–2884.
- Chen ML, McComb JG, Krieger MD. Atypical teratoid/rhabdoid tumors of the central nervous system: management and outcomes. *Neurosurg Focus*. 2005;18(6A):E8.
- Tekautz TM, Fuller CE, Blaney S, et al. Atypical teratoid/rhabdoid tumors (ATRT): improved survival in children 3 years of age and older with radiation therapy and high-dose alkylator-based chemotherapy. *J Clin Oncol*. 2005;23(7):1491–1499.

7. Chi SN, Zimmerman MA, Yao X, et al. Intensive multimodality treatment for children with newly diagnosed CNS atypical teratoid rhabdoid tumor. *J Clin Oncol*. 2009;27(3):385–389.
8. Sultan I, Qaddoumi I, Rodriguez-Galindo C, Nassan AA, Ghandour K, Al-Hussaini M. Age, stage, and radiotherapy, but not primary tumor site, affects the outcome of patients with malignant rhabdoid tumors. *Pediatric Blood & Cancer*. 2010;54(1):35–40.
9. Kordes U, Gesk S, Fruhwald MC, et al. Clinical and molecular features in patients with atypical teratoid rhabdoid tumor or malignant rhabdoid tumor. *Genes Chromosomes Cancer*. 2010;49(2):176–181.
10. Bruggers CS, Bleyl SB, Pysher T, et al. Clinicopathologic comparison of familial vs sporadic atypical teratoid/rhabdoid tumors (AT/RT) of the central nervous system. *Pediatr Blood Cancer*. 2010;56(7):1026–1031.
11. Freije WA, Castro-Vargas FE, Fang Z, et al. Gene expression profiling of gliomas strongly predicts survival. *Cancer Res*. 2004;64(18):6503–6510.
12. Jones DT, Mulholland SA, Pearson DM, et al. Adult grade II diffuse astrocytomas are genetically distinct from and more aggressive than their paediatric counterparts. *Acta Neuropathologica*. 2011;121(6):753–761.
13. Kool M, Koster J, Bunt J, et al. Integrated genomics identifies five medulloblastoma subtypes with distinct genetic profiles, pathway signatures and clinicopathological features. *PLoS ONE*. 2008;3(8):e3088.
14. Northcott PA, Korshunov A, Witt H, et al. Medulloblastoma Comprises Four Distinct Molecular Variants. *J Clin Oncol*. 2010;29(11):1408–1414.
15. Phillips HS, Kharbanda S, Chen R, et al. Molecular subclasses of high-grade glioma predict prognosis, delineate a pattern of disease progression, and resemble stages in neurogenesis. *Cancer Cell*. 2006;9(3):157–173.
16. Pomeroy SL, Tamayo P, Gaasenbeek M, et al. Prediction of central nervous system embryonal tumour outcome based on gene expression. *Nature*. 2002;415(6870):436–442.
17. Thompson MC. Genomics identifies medulloblastoma subgroups that are enriched for specific genetic alterations. *J Clin Oncol*. 2006;24(12):1924–1931.
18. Gravendeel LAM, Kouwenhoven MCM, Gevaert O, et al. Intrinsic gene expression profiles of gliomas are a better predictor of survival than histology. *Cancer Res*. 2009;69(23):9065–9072.
19. Nutt CL, Mani DR, Betensky RA, et al. Gene expression-based classification of malignant gliomas correlates better with survival than histological classification. *Cancer Res*. 2003;63(7):1602–1607.
20. Charboneau A, Chai J, Jordan J, et al. P-Akt expression distinguishes two types of malignant rhabdoid tumors. *J Cell Physiol*. 2006;209(2):422–427.
21. Birks DK, Kleinschmidt-DeMasters BK, Donson AM, et al. Claudin 6 is a positive marker for atypical teratoid/rhabdoid tumors. *Brain Pathol*. 2010;20(1):140–150.
22. Ma HI, Kao CL, Lee YY, et al. Differential expression profiling between atypical teratoid/rhabdoid and medulloblastoma tumor in vitro and in vivo using microarray analysis. *Childs Nerv Syst*. 2010;26(3):293–303.
23. Wu Z, Irizarry R, Gentleman R, Martinez MF, Spencer F. A model-based background adjustment for oligonucleotide expression arrays. *J Am Stat Assoc*. 2004;99:909–917.
24. Smyth GK. Linear models and empirical bayes methods for assessing differential expression in microarray experiments. *Stat Appl Genet Mol Biol*. 2004;3:Article3.
25. Dennis G, Jr., Sherman BT, Hosack DA, et al. DAVID: Database for Annotation, Visualization, and Integrated Discovery. *Genome Biol*. 2003;4(5):P3.
26. Huang da W, Sherman BT, Lempicki RA. Systematic and integrative analysis of large gene lists using DAVID bioinformatics resources. *Nat Protoc*. 2009;4(1):44–57.
27. Ashburner M, Ball CA, Blake JA, et al. Gene ontology: tool for the unification of biology. The Gene Ontology Consortium. *Nat Genet*. 2000;25(1):25–29.
28. Subramanian A, Tamayo P, Mootha VK, et al. Gene set enrichment analysis: a knowledge-based approach for interpreting genome-wide expression profiles. *Proc Natl Acad Sci USA*. 2005;102(43):15545–15550.
29. Hasselblatt M, Bohm C, Tatenhorst L, et al. Identification of novel diagnostic markers for choroid plexus tumors: a microarray-based approach. *Am J Surg Pathol*. 2006;30(1):66–74.
30. Sevenet N, Lellouch-Tubiana A, Schofield D, et al. Spectrum of hSNF5/INI1 somatic mutations in human cancer and genotype-phenotype correlations. *Hum Mol Genet*. 1999;8(13):2359–2368.
31. Wyatt-Ashmead J, Kleinschmidt-DeMasters B, Mierau GW, et al. Choroid plexus carcinomas and rhabdoid tumors: phenotypic and genotypic overlap. *Pediatr Dev Pathol*. 2001;4(6):545–549.
32. Gessi M, Giangaspero F, Pietsch T. Atypical teratoid/rhabdoid tumors and choroid plexus tumors: when genetics “surprise” pathology. *Brain Pathol*. 2003;13(3):409–414.
33. Judkins AR, Burger PC, Hamilton RL, et al. INI1 protein expression distinguishes atypical teratoid/rhabdoid tumor from choroid plexus carcinoma. *J Neuropathol Exp Neurol*. 2005;64(5):391–397.
34. Schittenhelm J, Nagel C, Meyermann R, Beschoner R. Atypical teratoid/rhabdoid tumors may show morphological and immunohistochemical features seen in choroid plexus tumors [published online ahead of print January 30, 2011]. *Neuropathology* 2011; doi: 10.1111/j.1440-1789.2010.01189.x.
35. Pera EM, Ikeda A, Eivers E, De Robertis EM. Integration of IGF, FGF, and anti-BMP signals via Smad1 phosphorylation in neural induction. *Genes Dev*. 2003;17(24):3023–3028.
36. LaBonne C, Bronner-Fraser M. Neural crest induction in *Xenopus*: evidence for a two-signal model. *Development*. 1998;125(13):2403–2414.
37. Nguyen VH, Trout J, Connors SA, Andermann P, Weinberg E, Mullins MC. Dorsal and intermediate neuronal cell types of the spinal cord are established by a BMP signaling pathway. *Development*. 2000;127(6):1209–1220.
38. Currie DS. Direct and indirect roles of CNS dorsal midline cells in choroid plexus epithelia formation. *Development*. 2005;132(15):3549–3559.
39. Hebert JM, Mishina Y, McConnell SK. BMP signaling is required locally to pattern the dorsal telencephalic midline. *Neuron*. 2002;35(6):1029–1041.
40. Liem KF, Jr., Tremml G, Jessell TM. A role for the roof plate and its resident TGFβ-related proteins in neuronal patterning in the dorsal spinal cord. *Cell*. 1997;91(1):127–138.
41. Timmer JR, Wang C, Niswander L. BMP signaling patterns the dorsal and intermediate neural tube via regulation of homeobox and helix-loop-helix transcription factors. *Development*. 2002;129(10):2459–2472.
42. Gomes WA, Mehler MF, Kessler JA. Transgenic overexpression of BMP4 increases astroglial and decreases oligodendroglial lineage commitment. *Dev Biol*. 2003;255(1):164–177.
43. Gross RE, Mehler MF, Mabie PC, Zang Z, Santschi L, Kessler JA. Bone morphogenetic proteins promote astroglial lineage commitment by mammalian subventricular zone progenitor cells. *Neuron*. 1996;17(4):595–606.
44. Alder J, Lee KJ, Jessell TM, Hatten ME. Generation of cerebellar granule neurons in vivo by transplantation of BMP-treated neural progenitor cells. *Nat Neurosci*. 1999;2(6):535–540.

45. Angley C, Kumar M, Dinsio KJ, Hall AK, Siegel RE. Signaling by bone morphogenetic proteins and Smad1 modulates the postnatal differentiation of cerebellar cells. *J Neurosci.* 2003;23(1):260–268.
46. Kang JS, Alliston T, Delston R, Derynck R. Repression of Runx2 function by TGF-beta through recruitment of class II histone deacetylases by Smad3. *EMBO J.* 2005;24(14):2543–2555.
47. Ross S, Cheung E, Petrakis TG, Howell M, Kraus WL, Hill CS. Smads orchestrate specific histone modifications and chromatin remodeling to activate transcription. *EMBO J.* 2006;25(19):4490–4502.
48. Sun F, Chen Q, Yang S, et al. Remodeling of chromatin structure within the promoter is important for bmp-2-induced fgfr3 expression. *Nucleic Acids Res.* 2009;37(12):3897–3911.
49. Young DW, Pratap J, Javed A, et al. SWI/SNF chromatin remodeling complex is obligatory for BMP2-induced, Runx2-dependent skeletal gene expression that controls osteoblast differentiation. *Journal of Cellular Biochemistry.* 2005;94(4):720–730.
50. Liu B, Tian D, Yi W, et al. Effect of Bone Morphogenetic Protein 4 in the Human Brain Glioma Cell Line U251. *Cell Biochemistry and Biophysics.* 2010;58(2):91–96.
51. Zhao H, Ayrault O, Zindy F, Kim JH, Roussel MF. Post-transcriptional down-regulation of Atoh1/Math1 by bone morphogenic proteins suppresses medulloblastoma development. *Genes & Development.* 2008;22(6):722–727.
52. Rothhammer T, Poser I, Soncin F, Bataille F, Moser M, Bosserhoff AK. Bone morphogenic proteins are overexpressed in malignant melanoma and promote cell invasion and migration. *Cancer Res.* 2005;65(2):448–456.
53. Furuta Y, Piston DW, Hogan BL. Bone morphogenetic proteins (BMPs) as regulators of dorsal forebrain development. *Development.* 1997;124(11):2203–2212.
54. Krizhanovsky V, Ben-Arie N. A novel role for the choroid plexus in BMP-mediated inhibition of differentiation of cerebellar neural progenitors. *Mechanisms of Development.* 2006;123(1):67–75.
55. Gibson P, Tong Y, Robinson G, et al. Subtypes of medulloblastoma have distinct developmental origins. *Nature.* 2010;468(7327):1095–1099.
56. Sharma MK, Mansur DB, Reifenberger G, et al. Distinct genetic signatures among pilocytic astrocytomas relate to their brain region origin. *Cancer Res.* 2007;67(3):890–900.
57. Taylor MD, Poppleton H, Fuller C, et al. Radial glia cells are candidate stem cells of ependymoma. *Cancer Cell.* 2005;8(4):323–335.